

# Raman-induced gratings in atomic media

V. G. Arkhipkin\* and S. A. Myslivets

*L. V. Kirensky Institute of Physics, Krasnoyarsk 660036, Russia*

*\*Corresponding author: avg@iph.krasn.ru*

Received April 3, 2014; revised April 24, 2014; accepted April 24, 2014;  
posted April 25, 2014 (Doc. ID 209508); published May 26, 2014

A novel type of electromagnetically induced gratings based on the Raman nonlinearity in the field of standing pump waves are proposed. Unlike electromagnetically induced absorption gratings, these gratings are based on the spatial modulation of Raman susceptibility. We present a theoretical study of the optical response of such a spatial periodically modulated three-level atomic medium. It is shown that transmission and reflection of a probe Raman wave can be simultaneously amplified in the grating. Transmission and reflection spectra can be controlled by varying the pump field intensity. The basic mechanism responsible for all-optical control of transmission and reflection in the samples of Raman driven atoms are discussed. © 2014 Optical Society of America

OCIS codes: (190.2055) Dynamic gratings; (050.5298) Photonic crystals; (230.4320) Nonlinear optical devices.  
<http://dx.doi.org/10.1364/OL.39.003223>

Artificial periodic structures such as photonic crystals (PCs) offer unprecedented possibilities to control light propagation [1]. A large majority of PCs are formed by a periodic modulation of the refractive index, i.e., a modulation of the real part of the dielectric constant. The periodic variation of the refractive index leads to Bragg scattering of light, and electromagnetic wave propagation becomes best described in terms of a photonic band structure, akin to the electronic band structure in a crystalline solid. When the incident light wavevector is close to the Brillouin zone boundary the propagation of light is strongly affected, leading to the existence of a range of frequencies for which light does not propagate, named as a photonic bandgap (PBG) [2]. Additional functionality can be created by including absorbing features into the structure, thus creating PCs with complex dielectric indices [3,4]. The presence of absorption or gain can radically change the nature of wave propagation in such materials, including the very notion of forbidden and allowed bands [5]. An electromagnetically induced PBG material has also been devised in a semiconductor heterostructure with layers periodically doped with different atomic densities. Nonlinear optical excitations of these atoms create a periodic refractive index contrast that leads to a PBG [6].

Quite a distinct approach to PCs uses optical resonant or quasi-resonant nonlinearities that can be induced in a multilevel medium. Such nonlinearities can be exploited to generate spatially periodic structures required to devise an optically tunable PBG. Unlike standard PCs, here a periodic structure is created by external control light beams. Novel photonic structures with a tunable PBG could be created by optically inducing coherent nonlinearities based on electromagnetically induced transparency (EIT) [7]. A standing wave driving configuration has been proposed to induce spatially periodic quantum coherence for both the generation of PBG [8–13] and the dynamic generation of stationary light pulses [14,15]. These structures are also referred to as electromagnetically induced absorption grating (EIAG) [16].

However, weakly driven EIT-based schemes still have some inherent drawbacks, one of which is that the probe field usually suffers significant attenuation and distortion at room temperature. Wave propagation in resonant optical media with an active Raman gain (ARG) has also

attracted considerable theoretical and experimental interest [17–20]. Unlike the EIT-based scheme, which is inherently absorptive, the central idea of the ARG scheme is that the probe field operates in a stimulated Raman emission mode, and hence can eliminate signal attenuation and subluminal (slow light) as well as superluminal (fast light) propagation of optical waves can be realized [18–20]. Recently, it has been shown that a gain-assisted giant Kerr effect [21,22] and superluminal solitons [23] can be obtained using an ARG medium. In [24–26] it was theoretically shown how one could use an ARG medium together with a PC cavity to create all-optical switches and transistors.

In this Letter we report on an alternative scheme to realize a dynamically variable periodic structure in an atomic medium based on the Raman effect in a standing pump wave configuration. A Raman-induced grating (RIG) is created in a three-level system when a weak probe beam and a strong pump wave interact with a Raman transition. Transmission and reflection of the probe beam can be greatly amplified owing to spatially modulated Raman gain regions where amplification occurs at the peaks of the standing wave pump field. Transmission and reflection peaks can be controlled by varying the pump field intensity. We emphasize that RIG is fundamentally different from the EIAG [16].

The atomic system under consideration is a standard active Raman scheme [Fig. 1(a)]. We consider an ensemble of identical lifetime broadening three-level atoms initially prepared in ground state  $|0\rangle$ . The transitions  $|0\rangle - |1\rangle$  and  $|1\rangle - |2\rangle$  are electric dipole allowed, and the transition  $|0\rangle - |2\rangle$  is electric dipole forbidden. The states  $|0\rangle$  and  $|1\rangle$  are coupled by a standing pump wave that is formed by two monochromatic counter-propagating pump fields  $E_p = 1/2\{E_{1p} \exp[-i(\omega_1 t - k_1 z)] + E_{2p} \exp[-i(\omega_1 t + k_1 z)]\}$ , where  $E_{1p}$  and  $E_{2p}$  are the amplitudes of fields with frequency  $\omega_1$  and wave vector  $k_1$ . For simplicity, we assume that the amplitudes are real and  $E_{1p} = E_{2p} = E_1$ . In this case,  $E_p = E_1 \exp[-i(\omega_1 t)] \cos(k_1 z)$  and a Rabi frequency of the pump standing wave can be written as  $\Omega_p = \Omega_1 \cos(k_1 z)$ , where  $\Omega_1 = d_{01} E_1 / \hbar$ . A weak probe Raman wave  $E_s = 1/2 E_2 \exp[-i(\omega_2 t - k_2 z)]$  ( $|E_2| \ll |E_1|$ ) also propagates along the  $z$  direction and interacts with the

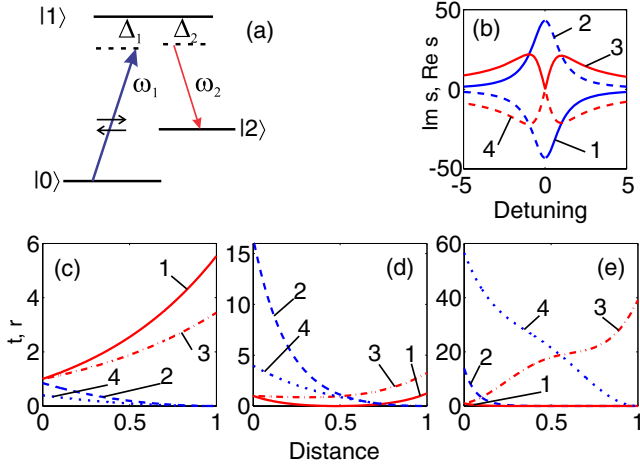


Fig. 1. (a) Energy-level diagram for a Raman scheme driven by a standing wave pump  $\omega_1$  and a traveling wave probe  $\omega_2$ . (b) Imaginary and real parts of  $\pm s(\omega_2)$  versus scaled Raman detuning  $\Delta_{20}/\gamma_{20}$  for the pump Rabi frequency  $\Omega_1/\gamma_{10}$ . 1 –  $\text{Im}(s)$ , 2 –  $\text{Im}(-s)$ , 3 –  $\text{Re}(s)$ , 4 –  $\text{Re}(-s)$ . (c)–(e) Spatial intensity distribution of the forward  $t$  (1,3) and backward  $r$  (2,4) probe components inside a sample of length  $L \simeq 0.6$  mm for various pump Rabi frequencies and Raman detunings. (c)  $\Omega_1 = 0.5\gamma_{10}$ , 1, 2 –  $\Delta_{20} = 0$ , and 3, 4 –  $\Delta_{20} = \gamma_{20}$ , (d)  $\Omega_1 = \gamma_{10}$ , 1, 2 –  $\Delta_{20} = 0$ , and 3, 4 –  $\Delta_{20} = 0.95\gamma_{20}$ , and (e)  $\Omega_1 = 1.7\gamma_{10}$ , 1, 2 –  $\Delta_{20} = 0$  and 3, 4 –  $\Delta_{20} = 2\gamma_{20}$ .  $\Delta_1 = 30\gamma_{10}$ , other parameters are listed in the text.

transition  $|1\rangle - |2\rangle$ . Both fields are detuned from the state  $|1\rangle$  with a large one-photon detuning. An off-resonant standing pump field couples the  $|0\rangle - |1\rangle$  transition and a medium with spatially modulated nonlinear dielectric permeability is created by Raman nonlinearity. The probe being weak, levels  $|1\rangle$  and  $|2\rangle$  remain empty, and the space distribution of atoms remains homogeneous within the sample. Owing to periodic spatial modulation induced by the standing wave, the weak probe wave propagates as in a one-dimensional grating with periodicity  $a = \lambda_1/2$ . The refractive index experienced by the probe Raman wave can be described by a dielectric function

$$\begin{aligned} \varepsilon_2(z) &= 1 + 4\pi N\chi_2 + 4\pi N\chi_R|E_1|^2 \cos^2(k_1 z) \\ &= \varepsilon_{20} + \Delta\varepsilon(1 + \cos(2k_1 z)), \end{aligned} \quad (1)$$

where  $\varepsilon_{20} = 1 + 4\pi N\chi_2$ ,  $\chi_2$  is the off-resonant linear susceptibility for a probe field,  $N$  is the concentration of atoms,  $\Delta\varepsilon = 2\pi\chi_R N|E_1|^2$ , and  $\chi_R$  is the Raman susceptibility [27]

$$\chi_R = \frac{1}{4\hbar^3} \frac{d_{21}^2 d_{10}^2}{\Delta_1^2 (\Delta_{20} + i\gamma_{20})}. \quad (2)$$

Here,  $\Delta_{20} = \Delta_1 - \Delta_2 = \omega_{20} - (\omega_1 - \omega_2)$  is the Raman detuning,  $\Delta_{1,2} = \omega_{10,12} - \omega_{1,2}$  are the one-photon detunings,  $\omega_{10}$  and  $\omega_{12}$  are the frequencies of atomic transitions,  $\gamma_{20}$  is the Raman transition half-width,  $d_{ij}$  is the matrix dipole moment of the transition, and  $\hbar$  is the reduced Planck constant. Formula (2) is valid when  $|\Delta_1| \gg |\Omega_1|, \gamma_{10}$ , and  $\gamma_{10}$  is the transition  $|1\rangle - |0\rangle$  half-width. It is essential that  $\text{Im}\chi_R < 0$ , i.e., the probe wave is gained (a negative

absorption) due to energy transfer from the pump to the probe field. The real part of  $\chi_R$  has normal dispersion near the resonance, therefore the group velocity can be much less than the velocity of light in vacuum [18,25]. It should be noted that  $|\Delta\varepsilon| \ll 1$ , which corresponds to a shallow depth of modulation (weak inhomogeneity of the dielectric constant). When  $\Delta_{20} \neq 0$  a hybrid grating is induced in a medium: gain grating and refraction grating.

Let us consider normal incidence of a weak probe wave on one-dimensional periodic medium with the permittivity of Eq. (1). A sample of finite length  $L$  contains a very large number of periods  $a$ . The wave equation for electric field strength  $E_2(z)$  inside a medium with a spatially modulated dielectric constant has the form [28]

$$\frac{d^2 E_2}{dz^2} + k_{20}^2 \varepsilon_2(z) E_2 = 0. \quad (3)$$

Considering Eq. (1), Eq. (3) can be reduced to the form

$$\frac{d^2 E_2}{dz^2} + k_2^2 [1 + \beta(1 + \cos 2k_1 z)] E_2 = 0, \quad (4)$$

where  $k_{20} = \omega_2/c$ ,  $k_2^2 = k_{20}^2 \varepsilon_{20}$ ,  $\beta = \Delta\varepsilon/\varepsilon_{20}$ , and  $c$  is the velocity of light in vacuum.

By using the method of coupled waves [28], the solution of Eq. (4) can be represented as a superposition of two waves propagating in opposite directions

$$E_2(z) = A(z)e^{ik_2 z} + B(z)e^{-ik_2 z}, \quad (5)$$

where  $A(z)$  and  $B(z)$  are the amplitudes of the forward and the backward wave, respectively. By substituting Eq. (5) into Eq. (4) and using the slowly varying amplitudes approximation  $k_2 dE_2/dz \gg d^2 E_2/dz^2$ , we obtain a system of two coupled equations for  $A(z)$  and  $B(z)$

$$\frac{dA}{dz} = i\alpha A + i\sigma B e^{i2\Delta k z}, \quad \frac{dB}{dz} = -i\alpha B - i\sigma A e^{-i2\Delta k z}, \quad (6)$$

where  $\alpha = k_2\beta/2$ ,  $\sigma = k_2\beta/4$ ,  $\Delta k = k_1 - k_2$ .

Linearly independent solutions of Eqs. (6) are proportional to  $\exp(\pm isz)$ , where  $s = \sqrt{(\Delta k - \alpha)^2 - \sigma^2}$ . The probe field  $E_2(z)$  in the layer is made of two counterpropagating waves  $E_2^+$  (forward) and  $E_2^-$  (backward). Their amplitudes are modulated with the frequency  $s$

$$E_2^+(z) = e^{ik_1 z} (a_1 e^{isz} + a_2 e^{-isz}), \quad (7)$$

$$E_2^-(z) = e^{-ik_1 z} (b_1 e^{-isz} + b_2 e^{isz}), \quad (8)$$

$$\kappa(\omega_2) = k_1 \pm s = k_1 \pm \sqrt{(\Delta k - \alpha)^2 - \sigma^2}. \quad (9)$$

Here,  $a_{1,2}$  and  $b_{1,2}$  are the constants of integration, which are determined by the boundary conditions, and  $\kappa(\omega_2)$  is the wave vector. Equations (7) and (8) define the linearly independent solutions or normal waves in the approximation  $|\Delta\varepsilon| \ll 1$  and  $|\Delta k| \ll |k_2|$ . The forward and

backward waves are a superposition of two spatial harmonics which may interfere with each other as follows from Eqs. (7) and (8). In general, the normal waves are inhomogeneous: they are damped or amplified. Expression (9) for  $\kappa(\omega_2)$  defines the dispersion relation.

Let us define the transmission and reflection coefficients for a layer of length  $L$ . Since  $|\Delta\epsilon| \ll 1$ , we can neglect the Fresnel reflection from the layer boundaries and take into account only the volume reflection. Then the boundary conditions can be written as  $E_2^+(0) = A_0$ ,  $E_2^-(L) = 0$ , where  $A_0$  is the incident probe wave amplitude. By using these boundary conditions we find the integration constants

$$a_{1,2} = A_0[s \mp (\Delta k - \alpha)]e^{\mp isL}/2D, \quad (10)$$

$$b_{1,2} = \pm iA_0\sigma e^{\pm isL}/2D, \quad (11)$$

where  $D = s \cos(sL) + i(\Delta k - \alpha) \sin(sL)$ . We introduce the notation  $t(z) = |E_2^+(z)|^2/|A_0|^2$  and  $r(z) = |E_2^-(z)/A_0|^2$ . By using Eqs. (7)–(11), one obtains

$$t(z) = |[s \cos s(L-z) + i(\Delta k - \alpha) \sin s(L-z)]/D|^2, \quad (12)$$

$$r(z) = |[\sigma \sin s(L-z)]/D|^2. \quad (13)$$

$t(z)$  and  $r(z)$  are the scaled intensities of the forward and backward probe components across a sample, respectively. Note that  $t(L) = T$  is the transmittance (or the amplification factor) and  $r(0) = R$  is the reflectance. To be definite, for numerical simulations we use parameters appropriated to the  $D_1$  line of Na atoms, in which case  $|0\rangle$  and  $|2\rangle$  are long-lived hyperfine sublevels of the electronic ground state  $3S_{1/2}$ . The atomic parameters are  $\gamma_{10} = 2\pi \cdot 10$  MHz,  $\gamma_{20} = \gamma_{10}/100$ , and  $N = 10^{12}$  cm $^{-3}$ .

Typical plots of  $\text{Im}\kappa(\omega_2) = \text{Im}s(\omega_2)$  and  $\text{Re}s(\omega_2)$  are shown in Fig. 1(b). Note that qualitative behavior of  $\text{Im}s(\omega_2)$  and  $\text{Re}s(\omega_2)$  does not depend on the Rabi frequency of the pump. The only effect of the increased pump is quantitative changes. In the frequency range  $\Delta_{20} < 0$ , the imaginary part  $\text{Im}s > 0$  and  $\text{Im}(-s) < 0$ . The situation is reverse for  $\Delta_{20} > 0$ . There is a jump in the change of  $\text{Im}s$  and  $\text{Im}(-s)$  while going through the resonance. It can be seen that there is no PBG, unlike the cases of EIT in the standing wave field [13] and the refractive index modulation [9,28]. Figures 1(c)–1(e) show the intensities of forward and backward probe waves in the sample as a function of the  $z/L$  coordinate. Their behavior is strongly dependent on the Raman detuning and the pump intensity for the given length of the sample. In Fig. 2, the normalized amplitudes  $A_{1,2} = |a_{1,2}e^{\pm isz}|/A_0$  and phases  $\varphi_{1,2}/\pi$  are given as a function of the  $z/L$  coordinate inside the sample for the forward wave  $E_2^+$ . It is seen that one of amplitudes increases while the other one decreases, and they may be in phase or in antiphase.

In Figs. 3(a)–3(c), the transmission  $T$  and reflection  $R$  for the probe are plotted as functions of the Raman detuning for different Rabi frequency  $\Omega_1$  of the pump field. We fix the one-photon detuning of the pump field and tune  $\Delta_2$ . The transmitted and reflected light can

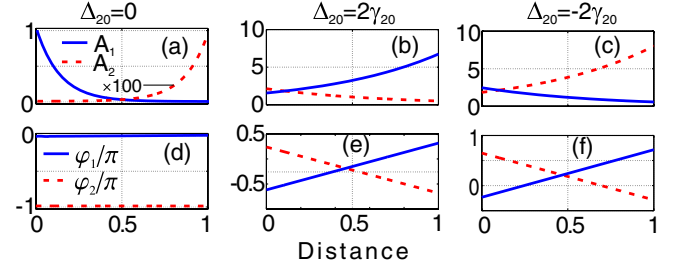


Fig. 2. (a)–(c) Spatial distribution of the amplitude  $A_{1,2}$ , and (d)–(f) phase  $\varphi_{1,2}$  of spatial harmonics for the forward probe wave inside a sample for frequency detunings corresponding to the Raman resonance  $\Delta_{20} = 0$  and transmission peaks  $\Delta_{20} = \pm 2\gamma_{20}$  when  $\Omega_1 = 1.7\gamma_{10}$ . Other parameters are the same as in Fig. 1.

be simultaneously amplified in some frequency range depending on the pump intensity. When  $|\Omega_1|/\gamma_{10} < 1$  the transmission and reflection signal has a maximal amplitude at the frequency corresponding to the Raman resonance. The transmission and reflection bands tend to split with growing pump intensity. In the region between peaks the transmission can be next to zero while the reflection can be greater than 1 and away from the Raman resonance  $T \rightarrow 1$  and  $R \rightarrow 0$ . Thus, near Raman resonance the amplitudes of forward and backward waves are amplified or damped, whereas away from the resonance the sample becomes transparent. The main contribution to the transmitted and reflected wave comes from one of the spatial harmonics, as it is seen in Figs. 3(d) and 3(e). An asymmetry of peaks in transmission and reflection with respect to  $\Delta_{20}$  is also observed [Fig. 3(c)] and it is sensitive to the intensity of pump field.

Figure 4 shows that the transmission and reflection drastically depend on the pump intensity. One can see that the small variations of the pump intensity can change the system from a transparent state to opaque one. Such controllable transmission is well suited for studies of all-optical switching at low pump light intensity.

In conclusion, we have theoretically demonstrated an electromagnetically induced grating based on the spatial modulation of Raman susceptibility in an atomic medium. The grating is created in a three-level atomic

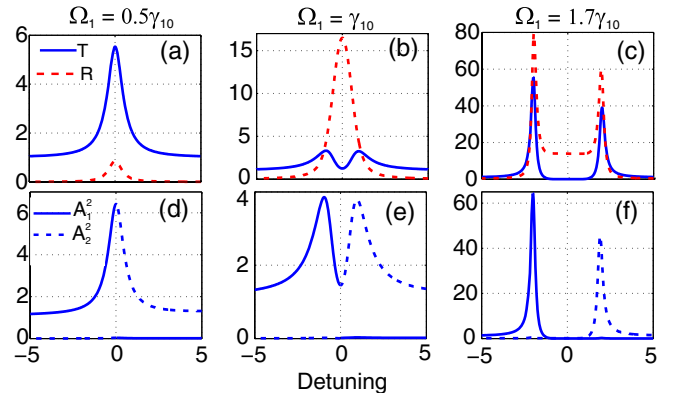


Fig. 3. (a)–(c) Reflection and transmission spectra as a function of scaled Raman detuning  $\Delta_{20}/\gamma_{20}$  for the different pump Rabi frequencies  $\Omega_1$ . (d)–(f) Normalized intensities of spatial harmonics  $A_1^2$  and  $A_2^2$  at the output of the sample for the forward wave.

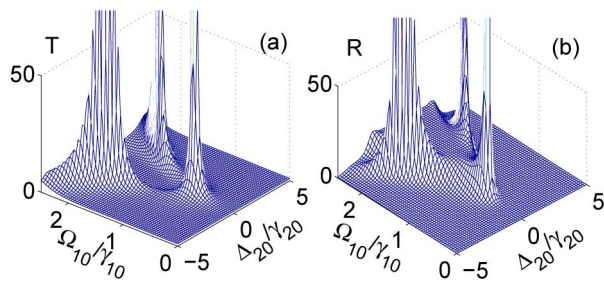


Fig. 4. (a) Transmission and (b) reflection versus the Raman detuning and pump Rabi frequency.

system when the pump field is a standing wave. Transmission and reflection can be amplified simultaneously and also dynamically tuned by varying the intensity of the pump field. The pump wave intensity required for these effects to be observed depends on a number of factors (one-photon pump frequency detuning, Raman resonance width, and the length of the medium) and can be anything from 10 to 100 mW/cm<sup>2</sup>. The results obtained are in good agreement with exact calculations based on the recurrence-relations technique [29]. For experimental realization both room-temperature and ultracold atoms and also molecular gases can be used. These experiments are similar to [16]. Hollow-core PC fibers filled by atoms can be used to reduce the pump intensity requirements. For many potential applications, solid-states are preferred. For the implementation of RIG at low pump the materials with long-lived coherence at Raman transition are needed. Praseodymium-doped Y<sub>2</sub>SiO<sub>5</sub> and diamond containing nitrogen vacancy color centers where EIT was observed [13] satisfy the specified condition, and therefore may be of interest for the experimental verification of RIG.

This work was supported in part by the RAS Grant No. 24.31, by SB RAS Grant Nos. 43 and 101, and by NSC of Taiwan and SB RAS through a joint project.

## References

1. C. Denz, S. Flach, and Y. S. Kivshar, eds., *Nonlinearities in Periodic Structures and Metamaterials* (Springer-Verlag, 2009), Vol. 150.
2. J. D. Joannopoulos, S. G. Johnson, J. N. Winn, and R. D. Meade, *Photonic Crystals: Molding the Flow of Light*, 2nd ed. (Princeton University, 2008).
3. M. Artoni, G. La Rocca, and F. Bassani, *Phys. Rev. E* **72**, 046604 (2005).
4. I. Gabitov, A. O. Korotkevich, A. I. Maimistov, and J. B. McMahon, "Coherent optical pulse dynamics in nanocomposite plasmonic Bragg gratings," arXiv:nlin/0702035 [nlin.PS] (2007).
5. N. N. Rozanov, S. V. Fedorov, R. S. Save'ev, A. A. Sukhorukov, and Y. S. Kivshar, *J. Exp. Theor. Phys.* **114**, 782 (2012).
6. Y. V. Rostovtsev, A. B. Matsko, and M. O. Scully, *Phys. Rev. A* **60**, 712 (1999).
7. M. Fleischhauer, A. Imamoglu, and J. P. Marangos, *Rev. Mod. Phys.* **77**, 633 (2005).
8. A. André and M. D. Lukin, *Phys. Rev. Lett.* **89**, 143602 (2002).
9. X. M. Su and B. S. Ham, *Phys. Rev. A* **71**, 013821 (2005).
10. M. Artoni and G. C. La Rocca, *Phys. Rev. Lett.* **96**, 073905 (2006).
11. S.-q. Kuang, R.-g. Wan, P. Du, Y. Jiang, and J.-y. Gao, *Opt. Express* **16**, 15455 (2008).
12. J.-H. Wu, G. C. La Rocca, and M. Artoni, *Phys. Rev. B* **77**, 113106 (2008).
13. J.-H. Wu, A. Raczynski, J. Zaremba, S. Zielinska-Kaniasty, M. Artoni, and G. La Rocca, *J. Mod. Opt.* **56**, 768 (2009).
14. M. Bajcsy, A. S. Zibrov, and M. D. Lukin, *Nature* **426**, 638 (2003).
15. K. R. Hansen and K. Molmer, *Phys. Rev. A* **75**, 053802 (2007).
16. A. W. Brown and M. Xiao, *Opt. Lett.* **30**, 699 (2005).
17. A. Dogariu, A. Kuzmich, and L. J. Wang, *Phys. Rev. A* **63**, 053806 (2001).
18. M. G. Payne and L. Deng, *Phys. Rev. A* **64**, 031802 (2001).
19. K. J. Jiang, L. Deng, and M. G. Payne, *Phys. Rev. A* **74**, 041803 (2006).
20. K. J. Jiang, L. Deng, and M. G. Payne, *Phys. Rev. A* **76**, 033819 (2007).
21. L. Deng and M. G. Payne, *Phys. Rev. Lett.* **98**, 253902 (2007).
22. G. S. Agarwal and S. Dasgupta, *Phys. Rev. A* **70**, 023802 (2004).
23. C. Hang and G. Huang, *Opt. Express* **18**, 2952 (2010).
24. V. G. Arkhipkin and S. A. Myslivets, *Phys. Rev. A* **80**, 061802 (2009).
25. V. G. Arkhipkin and S. A. Myslivets, *J. Exp. Theor. Phys.* **111**, 898 (2010).
26. V. G. Arkhipkin and S. A. Myslivets, *Phys. Rev. A* **88**, 033847 (2013).
27. R. W. Boyd, *Nonlinear Optics* (Academic, 1992).
28. S. Rautian, *Opt. Spectrosc.* **104**, 112 (2008).
29. V. G. Arkhipkin and S. A. Myslivets, *Quantum Electron.* **39**, 157 (2009).